Published in final edited form as:
Anal Biochem. 2010 March 15; 398(2): 203–211. doi:10.1016/j.ab.2009.12.020.

Identification of Inhibitors of V-ATPase Pumps in Yeast by HTS Flow Cytometry

Rebecca M. Johnson[1,4], **Chris Allen**[3,4], **Sandra D. Melman**[1], **Anna Waller**[3], **Susan M. Young**[3], **Larry A. Sklar**[2,3], and **Karlett J. Parra**[1,*]

[1]Department of Biochemistry and Molecular Biology University of New Mexico School of Medicine, Albuquerque, NM 87131, U.S.A.

[2]Department of Pathology and Cancer Center University of New Mexico School of Medicine, Albuquerque, NM 87131, U.S.A.

[3]Center for Molecular Discovery University of New Mexico School of Medicine, Albuquerque, NM 87131, U.S.A.

Abstract

Fluorescence intensity of the pH-sensitive carboxyfluorescein derivative BCECF was monitored by high throughput flow cytometry in living yeast cells. We measured fluorescence intensity of BCECF trapped in yeast vacuoles, acidic compartments equivalent to lysosomes where V-ATPases are abundant. Because V-ATPases maintain a low pH in the vacuolar lumen, V-ATPase inhibition by concanamycin A alkalinized the vacuole and increased BCECF fluorescence. Likewise, V-ATPase deficient mutant cells had greater fluorescence intensity than wild-type cells. Thus, we detected an increase of fluorescence intensity after short-term and long-term inhibition of V-ATPase function. We used yeast cells loaded with BCECF to screen a small chemical library of structurally diverse compounds in order to identify V-ATPase inhibitors. One compound, disulfiram, enhanced BCECF fluorescence intensity (although to a degree beyond anticipated for pH changes alone in the mutant cells). Once confirmed by dose response assays (EC_{50}=26 μM), we verified V-ATPase inhibition by disulfiram in secondary assays which measured ATP hydrolysis in vacuolar membranes. The inhibitory action of disulfiram against V-ATPase pumps revealed a novel effect previously unknown for this compound. Because V-ATPases are highly conserved, new inhibitors identified could be used as research and therapeutic tools in cancer, viral infections, and other diseases where V-ATPases are involved.

Keywords

Flow cytometry; BCECF; fluorescence; high throughput; chemical library; yeast; vacuoles; pH; V-ATPase; pumps; V-ATPase inhibitors; disulfiram; concanamycin A

*Corresponding Author. Department of Biochemistry and Molecular Biology University of New Mexico School of Medicine 1 University of New Mexico MSC08 4670 Albuquerque, NM 87131, USA *Phone*: 1 505 272 1633; FAX: 1 505 272 6587. kjparra@salud.unm.edu.
[4]Authors contributed equally to this work.

INTRODUCTION

V-ATPases[5] are conserved proton pumps important for pH homeostasis [1,2]. Located at the membrane of lysosomes, vacuoles and endosomes, V-ATPases sustain the acidic luminal pH needed for protein sorting and degradation, and for entry of viruses and bacterial toxins into host cells [1]. Cells specialized for active proton secretion such as kidney and bone, express V-ATPases at the plasma membrane where they fine-tune, respectively, the systemic acid-base balance and bone resorption [3,4]. Genetic mutations in V-ATPase subunit isoforms that are preferentially expressed in bone, kidney, and internal ear cause osteoporosis, distal renal tubular acidosis, and sensorineural deafness, respectively [6,7]. Each of these human conditions is characterized by abnormal cellular and systemic pH homeostasis.

V-ATPases are now recognized as novel anti-cancer targets. V-ATPases sustain the abnormal pH gradient that exists between the cytoplasm and the lumen of intracellular vesicles in malignant tumors [8,9]. In addition, V-ATPases generate an acid microenvironment that influences cancer progression, metastasis, and chemo-resistance [8–10]. Inhibition of V-ATPase activity in cancer cells results in abnormal pH (lysosomal alkalinization and cytosolic acidification), increased reactive oxygen species, and hypersensitivity to multiple drugs [11, 12]. Because V-ATPases are highly conserved pumps, lack of V-ATPase function triggers similar responses in cancer and yeast cells [13], yeast being the preferred model organism for the study of V-ATPases.

Most eukaryotes without functional V-ATPases die at early stages of development [14–16]; yet, complete lack of V-ATPase activity in yeast leads to a pH-dependent phenotype [13]. Yeast V-ATPase null mutants (*vma*Δ, vacuolar membrane ATPase) cannot grow at neutral pH and only grow at pH 5 [2]. Therefore, only yeast allows us to study the downstream consequences of blocking V-ATPase function simply by culturing the cells under conditions permissive for growth (medium adjusted to pH 5). Yeast *vma*Δ mutants cannot redistribute protons from the cytosol to the vacuole [17], the yeast compartment equivalent to mammalian lysosomes. As a result, yeast *vma*Δ mutants have greater vacuolar (pH_{vac}=6.9) and lower cytosolic (pH_{cyt}=5.7) pH than wild-type cells (pH_{vac}=5.6; pH_{cyt}=6.7) [17].

We developed a high throughput flow cytometry assay utilizing the environmental sensitivity of BCECF loaded into yeast vacuoles as a measurement tool. Because BCECF fluorescence signals increase as the pH increases, we hypothesized that BCECF fluorescence intensity will increase if yeast V-ATPases are inhibited because the vacuolar pH is alkalinized [17]. High throughput screening of a small collection of bioactive, structurally diverse compounds (880 off patent drug compounds) was performed in this study. We identified one hit: disulfiram. We confirmed its ability to increase the fluorescence intensity of yeast cells stained with BCECF by dose response assays *in vivo*, and verified its inhibitory effect on V-ATPase function by secondary assays conducted in vacuolar membrane fractions *in vitro*. This study is proof of principle that the assay can be used to identify novel V-ATPase inhibitors. Because yeast and mammalian V-ATPases have overlapping physiological roles [2,18], and share the same overall structure, subunit composition, and mechanisms of catalysis [1,2,18,20], V-ATPase inhibitors can be used as pharmacological tools to research the mechanisms controlling VATPases and pH homoeostasis from yeast to human.

[5]Abbreviations used: V-ATPase, vacuolar proton translocating ATPase; *vma*Δ, yeast vacuolar membrane ATPase null mutant strain; BCECF-AM, 2-,7-Bis(2-carboxyethyl)-5-(and-6)-carboxyfluorescein, acetoxymethyl ester; DMSO, dimethyl sulfoxide.

MATERIALS AND METHODS

Reagents

2-,7-Bis(2-carboxyethyl)-5-(and-6)-carboxyfluorescein, acetoxymethyl ester (BCECF-AM) was purchased from Invitrogen. Concanamycin A was purchased from Wako Biochemicals. Other chemicals were purchased from Sigma. BCECF, concanamycin A, and test compounds were stored as DMSO stocks. All reagents were diluted in aqueous buffer (or synthetic complete yeast medium, SD). The final concentration of DMSO in the assay was 0.5%.

Strains and Cell Growth

The wild-type strain BY4741 (*MATα his3Δ1 leu2Δ0 met15Δ0 ura3Δ0*; Open Biosystems) and the congenic *vma2*Δ::kanMX and *vma3*Δ::kanMX mutants were used throughout. Strains were a generous gift from Dr. Patricia Kane (SUNY Upstate Medical University, Syracuse, NY). Yeast cultures were grown overnight at 30° C to mid-log phase (0.5 Abs_{600}/ml) in YEPD medium (1% yeast extract, 1% bacto-peptone, 2% glucose) buffered to pH 5 with 50 mM sodium phosphate, 50 mM sodium succinate.

Flow Cytometry Sampling

Cells were resuspended in SD (synthetic complete) medium which consists of 0.67% yeast nitrogen base, supplemented with all required nutrients and amino acids and 2% glucose. A cell density of 0.1 – 0.3 Abs_{600}/ml was used in flow cytometry samples. This density was optimal in the 384-well format for 30 μl volumes (3–9 × 10^4 cells/well). We found greater cell density (0.5 –0.7 Abs_{600}/ml) slowed sampling through the cytometer. Best flow cytometry sampling and analysis results were obtained with uniform suspensions. Microplates were placed on an end-over-end rotator to maintain uniform suspensions during the incubations. Automated reading at the cytometer was done at room temperature. Each sample consisted of 2 μl taken from either a 30 μl well volume in the 384-wells format, or a 120 μl volume in the 96-well format. HyperCyt® sampling of a 384-well plate was completed in 10 min [21,22].

BCECF-AM Staining

Overnight cell cultures (0.5 Abs_{600}/ml) were harvested and washed once in SD medium. Cells were resuspended in SD (0.5 Abs_{600}/ml) treated with 50 μM (or 18 μM when indicated) BCECF-AM and incubated at 30 °C rocking for 30 min. Cells were harvested, excess BCECF-AM washed three times by centrifugation at 3,750 rpm for 10 min (Beckman GRP centrifuge) and resuspended in 20 ml SD medium. Labeling of cells with 18 μM and 50 μM BCECF-AM produced comparable signals. BCECF-AM was used at 50 μM for high throughput screen in order to ensure maximal assay sensitivity.

Concanamycin A Dose Response Flow Cytometry Assays

Wild-type cells were grown to mid-log phase, labeled with 18 μM BCECF-AM, washed, and resuspended in SD (1.0 Abs_{600}/ml), as described before. Cells were treated with 0, 1 μM, 2 μM, 3 μM, 5 μM, 10 μM, and 20 μM concanamycin A in the presence of 0.5% DMSO and incubated for 30 min at 30° C with rocking. For autofluorescence controls, unstained cells were resuspended in 0.5% DMSO alone or 0.5% DMSO containing 20 μM concanamycin A. Cells were harvested, and resuspended in SD containing the corresponding concentrations of concanamycin A, and distributed into 96-well plates, then diluted in SD (0.25 Abs_{600}/ml), and incubated at 30° C. For each concentration of concanamycin A tested, 6–8 replicates were measured. After excitation at 488 nm, fluorescent emissions were collected on a CYAN ADP (Beckman-Coulter) flow cytometer using a 530/40 nm filter set. Data files were processed using IDLQuery/HyperView software programs as describe below.

Dose Response Flow Cytometry Assays

Wild-type and *vma2*Δ cells were grown to mid-log phase and stained with 50 μM BCECF-AM as described above. Aliquots of 5 μl (0.5 Abs_{600}/ml) were distributed into 384-well plates containing an equal volume of 1:3 serial dilutions of test compounds (0.0015 – 2 mg/ml). Plates were incubated for 90 min at 30 °C. Flow cytometry (Excitation 488nm / Emissions 530/40 nm) was conducted as described above and data files processed using IDLQuery/HyperView software programs.

High Throughput Screen

Wild-type cells were grown to mid-log phase and labeled with 50 μM BCECF-AM. Aliquots of 15 μl volume (0.5 Abs_{600}/ml) were transferred to 384-well plates using liquid handling robots to which an equal volume of media containing 100 nl of 2 mg/ml test compounds (final concentration of ~6 ug/ml) was added. The final volume was 30 μl per well and the final concentration of DMSO was 0.5% in the screen. Microplates were configured with thirty-two control wells: column 1 containing wild-type cells treated with DMSO alone (negative control); and column 2 containing *vma2*Δ cells treated with DMSO alone (positive control). Thirty-two wash wells: columns 23 and 24 containing a diluted solution of detergent (0.015% Pluronic® F-68in SD medium). Test compounds were added to the remaining three hundred and twenty wells (columns 3 through 22). After addition of the test compounds, plates were incubated at 30 °C for 90 min and flow cytometry sampling started. Flow cytometry was conducted as described above and data files processed using IDLQuery/HyperView software programs.

Automated Data Analysis

Immediately after data acquisition by the flow cytometer, the IDLQuery/HyperView software program was used to analyze the data file. The program automatically detected the time-resolved data clusters (wells) and analyzed each to determine the median fluorescence intensity with excitation at 488 nm and emission collected using a 530/40 filter set [22]. Data were automatically exported to a Microsoft Excel spreadsheet that calculated the assay Z' factor [23]. This statistical parameter is used in high throughput screening for evaluating the quality of the assay and is calculated by using the equation:

$$Z' = 1 - (3 \times \text{STD of positive control} + 3 \times \text{STD of negative control}) / (|\text{mean of positive control} - \text{mean of negative control}|)$$

where STD is the standard deviation and the denominator is the absolute difference between the different controls. An assay with Z' value greater than 0.5 is acceptable for screening, i.e., consistent, significant difference between the controls are observed.

Secondary Assays

Vacuolar membranes were purified by flotation in one Ficoll gradient [24,25]. Briefly, three liters of wild-type yeast cells were grown overnight to 1–2 A_{600}/ml in YEPD pH 5 medium. Cells were harvested by centrifugation at 5,000 rpm in a GSA rotor, washed twice in 2% glucose, resuspended in 10 mM Tris·HCl, pH 7.5, containing 1.2 M sorbitol, and converted to spheroplasts by the addition of zymolase 100T (0.1 units/Abs_{600}). Spheroplasts were washed in YEPD pH 5 containing 1.2 M sorbitol and pellets subjected to osmotic lysis. Lysis was conducted by Dounce homogenization in lysis buffer (10 mM MES-Tris, pH 6.9, 0.1 mM $MgCl_2$, 12% Ficoll). The vacuolar fraction was floated by a 12% Ficoll gradient, converted to vacuolar membrane vesicles by dilution in 15 mM MES, pH 7, 4.8% glycerol buffer, and stored at −80 °C.

ATP hydrolysis was measured spectrophotometrically using an enzymatic assay coupled to oxidation of NADH [26] in the presence and absence of concanamycin A [27] and disulfiram.

Membranes (7 – 10 μg protein) were incubated with either disulfiram (0.91 – 167 μM) in the presence of 0.1% DMSO, concanamycin A (100 nM or 5 μM) in the presence of 0.1% DMSO, or 0.1% DMSO alone. After 10 min (or 5 min when indicated) on ice, samples were diluted 10-fold in ATPase reaction mixture (25 mM Tris.Acetate, pH 6.9, 25 mM KCl, 5 mM $MgCl_2$, 2mM ATP, 0.5 mM NADH, 2 mM phosphoenolpyruvate, 30 U/ml L-lactic dehydrogenase, 30 U/ml pyruvate kinase). ATP hydrolysis was measured spectrophotometrically at 340 nm [26]. Addition of an equal volume of DMSO (0.1% – 1%) and disulfiram (67 μM – 168 μM) directly into the ATPase reaction mixture had no effect on ATP hydrolysis. Protein concentration was measured as described by Lowry [28].

Confocal Microscopy

Yeast cells were grown to mid-log phase and labeled with BCECF as described above. Briefly, cells were treated with 18 μM BCECF-AM for 30 min at 30 °C, washed three times by centrifugation, and observed with a Zeiss LSM 510 Confocal Microscope at 63×DIC.

RESULTS

BCECF-AM is Trapped in Yeast Vacuoles

The fluorescent dye BCECF-AM is a pH indicator that serves as a vacuolar marker in living yeast cells because vacuoles are compartments rich in esterases where the acetoxymethyl ester group is hydrolyzed and BCECF trapped [17,29,30]. In order to verify its vacuolar localization, we visualized cells labeled with BCECF by fluorescence microscopy. Wild-type yeast cells (Fig. 1, *A*–*B*) were compared to two V-ATPase null mutants, *vma2*Δ (Fig. 1, *C*–*D*) and *vma3*Δ (not shown). Both mutants lack all V-ATPase activity, but the *vma2*Δ mutation deletes a subunit of the peripheral domain of the enzyme (subunit B), whereas the *vma3*Δ mutation deletes a proteolipid subunit of the membrane domain (subunit c) [2].

Images confirmed BCECF exclusive labeling of the vacuole (Fig. 1 *B* and *D*), which appeared as a depression under differential interference contrast microscopy (Fig. 1, *A* and *C*). Staining yeast cells with 18 μM and 50 μM BCECF-AM yielded comparable results indicating that at 18 μM BCECF-AM and above saturation was reached.

Flow Cytometry Measured BCECF Signals

Yeast cells impaired for V-ATPase activity have greater vacuolar pH than wild-type cells [17]. Because BCECF fluorescence intensity increases as the pH increases from 5 to 8 [31], we asked if BCECF trapped in yeast vacuoles could detect the more alkaline pH that exist in the vacuolar lumen of *vma* null mutants. The fluorescence of *vma2*Δ, *vma3*Δ, and an isogenic wild-type strain each stained with the vacuolar fluorophore was measured to determine if BCECF signals could be distinguished from background autofluorescence and whether mutants emitted brighter signals than wild-type cells (Fig. 2). Overnight cultures of each strain were harvested, resuspended in SD medium, and divided into two aliquots. One aliquot was incubated with 50 μM BCECF-AM in the presence of 0.5% DMSO, the other with an equal volume of 0.5% DMSO without BCECF-AM to serve as baseline or autofluorescence control. An additional autofluorescence control for wild-type cells was included, which had cells in SD without DMSO.

For wild-type cells (Fig. 2A), aliquots consisting of 30 μl were distributed into a 384-well plate (48 replicate wells) and read in a flow cytometer. After excitation at 488 nm, fluorescent emissions were collected using a 530/40 nm filter set. The median fluorescence intensity was calculated with IDLQuery/HyperView software and used for subsequent analysis. Fluorescence intensity of wild-type cells stained with BCECF was about 14-fold greater than unstained cells, indicating that the assay has a large signal-to-background ratio.

In addition, no change of fluorescence intensity was detected before and after addition of 0.5% DMSO to either un-stained or BCECF-stained cells. Therefore, DMSO, which is the solvent used to resuspend BCECF and other compounds throughout this study, neither emitted florescence nor interfered with BCECF fluorescence signals.

The fluorescence response exhibited a larger signal-to-background ratio of about 42-fold in V-ATPase null mutant cells. For *vma2*Δ and *vma3*Δ mutants, samples were taken separately six times from an Eppendorf tube (Fig. 2 *B*–*C*). Independent experiments showed BCECF fluorescence intensity three to five times brighter in *vma2*Δ and *vma3*Δ than wild-type cells. Because the vacuolar pH of *vma2*Δ and *vma3*Δ is ~1.3 units greater than wild-type cells [17], these results indicated that the assay detected the more alkaline pH that exists in vacuoles of cells impaired for V-ATPase proton transport.

As anticipated, *vma2*Δ and *vma3*Δ generated comparable results. Either *vma2*Δ or *vma3*Δ stained with BCECF can serve equally well as reference values of the maximum fluorescence intensity measured as yeast cells experience V-ATPase inactivation. Thus, either one of these two strains could be used as positive control in high throughput screens of chemical libraries when we search for inhibitors of V-ATPase pumps; we elected to use *vma2*Δ.

The results shown in Fig. 2B were extended to high throughput formats using 384-well plates (30μl/well). We analyzed wild-type and *vma2*Δ cells simultaneously. Wild-type and *vma2*Δ were compared after exposure to four different treatments: *i*) cells stained with BCECF resuspended in 0.5% DMSO, *ii*) cells stained with BCECF resuspended in SD medium, *iii*) cells unstained resuspended in 0.5% DMSO, and *iv*) cells unstained resuspended in SD medium. Three columns (48 replicates) were analyzed and pairs of treatments compared (Table 1). These experiments also revealed large signal-to-background ratios in wild-type and *vma2*Δ cells. Again, *vma2*Δ exhibited about three times larger BCECF fluorescence intensity than wild-type cells; and the assay was not sensitive to 0.5% DMSO, which did not interfere with BCECF fluorescence.

Next, we compared the fluorescence intensity of stained wild-type cells to *vma2*Δ cells each resuspended in 0.5% DMSO, because *vma2*Δ will be used as positive control in high throughput screens. By comparing the minimum (wild-type) and the maximum (*vma2*Δ) BCECF fluorescence intensities we calculated the Z' value for the dynamic range of the high throughput screening at 0.72. As judged by this statistical parameter, these experiments consistently demonstrated a tight data distribution reproducible from experiment-to-experiment and between plates.

Concanamycin A Modulates BCECF-AM Fluorescence

Yeast cells subjected to high throughput screens will experience a sudden loss of V-ATPase activity when incubated with pharmacological inhibitors of V-ATPase proton transport. In order to test the responsiveness of the assay to short-term inhibition of V-ATPase activity, we treated cells with a highly potent V-ATPase inhibitor, concanamycin A [27,32] and we monitored apparent pH-dependent fluorescence intensity changes.

Wild-type cells stained with BCECF were incubated with varied concentrations of the V-ATPase inhibitor at 30 °C for 30 min (Fig. 3A). Dose-response assays showed that at 1 μM concanamycin A and above, fluorescence intensity increased gradually indicating that concanamycin A inhibited the pump in a dose-dependent manner and the apparent vacuolar pH increased. Concanamycin A dose-dependent changes in fluorescence intensity were reproducible. The EC_{50} was estimated at 2.10 – 2.27 μM concanamycin A by three independent experiments. This is consistent with previous studies showing that at least 1 μM is necessary

to inhibit yeast V-ATPase activity *in vivo* [33–35]; although nanomolar concentrations of conacanmycin A are sufficient to inhibit V-ATPase in membrane fractions [27,32].

These results suggest that inhibition of V-ATPase by compounds that mimic the effects of concanamycin A will generate sufficiently ample changes in fluorescent signals to be detected in this assay. We consistently measured a large increase of fluorescence intensity after treating wild-type cells with 5 μM concanamycin A (Fig. 3B). At 5 μM concanamycin A the fluorescence intensity increased by about 3-fold (Z'=0.85 – 0.95), resembling *vma2*Δ and *vma3*Δ mutants. Time-course response experiments revealed stable BCECF fluorescence signals before and after treatment of wild-type cells with concanamycin A (Fig. 3C). We concluded that this assay can detect the apparently more alkaline vacuolar pH generated by pharmacological inhibition of V-ATPase pumps.

High Throughput Screen

In order to validate the assay for high throughput screen, we conducted a pilot screen using the Prestwick Chemical Library, which is a small collection of structurally diverse, bioactive compounds (880 off-patent drug compounds). Microplates were configured as shown in Fig. 4A. Controls involved wild-type (negative control) and *vma2*Δ (positive control) cells stained with BCECF. These controls defined, respectively, the lowest and highest fluorescence intensity measured in a V-ATPase dependent manner during the screening, and constituted the dynamic range of the assay.

Screening of the 880 compounds yielded Z' factors of 0.56 – 0.64 from plate-to-plate. Because the Z' factor is sensitive to the data variability as well as the signal dynamic range, these results further support the assay's suitability for high throughput screening. A representative result is shown in Fig. 4B. The dynamic range of the fluorescence intensity signal in the screen was between ~100 (negative control) to ~350 (positive control) hundred thousand fluorescein equivalents. Calculations of percent response were set to 100% at the positive control level and 0% at the negative control. Cutoffs were set at three times the standard deviation of the negative control (i.e., DMSO in Fig. 4A) which corresponded to a percent response of 43%. We identified 25 compounds that enhanced BCECF fluorescence intensity above this cutoff. Potential hit compounds were re-tested by confirmatory assays. Confirmatory assays included wild-type cells (unstained and stained) and *vma2*Δ cells (stained) to which incremental doses of the test compounds were added in parallel. Fourteen of these potential hits were classified as false positives because they failed to increase BCECF fluorescence intensity in the confirmatory dose response experiments. Ten of the remaining compounds enhanced fluorescence intensity of both wild-type and *vma2*Δ cells in a concentration dependent manner, indicating that mechanisms independent of V-ATPase function were likely responsible for their effect.

One compound, *disulfiram* (tetraethylthiuram disulfide), displayed V-ATPase dependent effects (Fig. 5). *Disulfiram* did not increase the fluorescence intensity of *vma2*Δ control cells within a broad range of concentrations tested in the confirmatory dose response experiments. The observation that 67 μM *disulfiram* increased fluorescence signals in *vma2*Δ by about 2.5-fold, suggests that *disulfiram* at very high concentrations could elevate BCECF fluorescence intensity via mechanisms that do not require V-ATPase function in living yeast cells. However, the magnitude of the increment of BCECF fluorescence intensity in *vma2*Δ was larger than expected based on the anticipated pH changes alone. Even so, a greater effect was observed in wild-type cells. *Disulfiram* increased the fluorescence intensity of wild-type cells up to 10-fold. Following treatment with *disulfiram*, wild-type cells reached signals comparable to *vma2*Δ cells (positive control) suggesting that the V-ATPase was inhibited and the apparent vacuolar pH increased. We calculated the EC_{50} to be 26 μM in two independent dose response experiments.

Finally, the inhibitory effect of this compound was validated by conducting secondary assays. We measured ATP hydrolysis directly in vacuolar membrane fractions treated with *disulfiram* (Fig. 6). Inhibition of ATPase activity was dose dependent with EC_{50}=24.75 (+/− 1.9) μM (Fig. 6A). Thus, the EC_{50} of *disulfiram* was about 10^4-fold greater than the EC_{50} of concanamycin A measured on membrane fractions [27]. As anticipated, greater concentrations of *disulfiram* than concanamycin A were necessary to inhibit V-ATPase activity (Fig. 6B). Nevertheless, the effect of *disulfiram* on ATP hydrolysis was V-ATPase specific. Pre-incubation with concanamycin A prior to addition of inhibitory concentrations of *disulfiram* to vacuolar membranes did not generate any additional inhibition of ATP hydrolysis, indicating that *disulfiram* acted by inhibiting V-ATPase pumps. We concluded that *disulfiram* discriminated between V-type ATPases (concanamycin A-sensitive) and other ATPases that co-exist at the yeast vacuolar membranes.

DISCUSSION

We used high throughput flow cytometry to monitor changes in BCECF fluorescence intensity in living yeast cells. By using the HyperCyt® platform technology, this approach interfaced a flow cytometer and autosampler for accurate quantitative measurements [21,22]. The main advantage of the HyperCyt® platform is the simplification of the technical effort associated with preparation of reagents for high throughput screening to a single step, loading yeast cells with a pH-sensitive fluorophore, while allowing us to monitor BCECF fluorescence changes in a manner dependent on V-ATPase activity.

High throughput screening of the Prestwick Chemical Library identified twenty five compounds which enhanced vacuolar BCECF fluorescence intensity by mechanisms potentially associated with V-ATPase activity. Potential hits were re-tested in dose response experiments. Because we added test compounds to wild-type and *vma2*Δ cells in parallel, confirmatory assays allowed us to discriminate compounds that acted by V-ATPase dependent and independent mechanisms. Ten compounds showed dose-dependent response in both wild-type cells and control *vma2*Δ cells suggesting that their stimulation of BCECF fluorescence intensity did not require V-ATPase activity. Fourteen compounds were classified as false positives because they failed to increase BCECF fluorescence intensity in the confirmatory assays.

One hit was confirmed, *disulfiram*, a drug used to treat alcoholism [36]. *Disulfiram* is a cysteine modifying compound [36] and our results indicated that this compound inhibited V-ATPase proton transport (Fig 5) as well as concanamycin A-sensitive ATP hydrolysis (Fig. 6). Although further studies will be required to establish its mechanism of action, *disulfiram* could act by inhibiting ATP hydrolysis at the catalytic domain of the enzyme. ATP hydrolysis by VATPases is blocked by disulfide bond formation between cysteine residues near the catalytic site [37, 38]. It is possible that *disulfiram* acts by modifying the cysteine in the P-loop of the catalytic subunit (subunit A), which is also the site of inhibition by N-N-Ethylmaleimide (NEM) [37, 38], another thiol reactive compound. Independent lines of evidence further support the notion that *disulfiram* can inhibit V-ATPase function. *Disulfiram* has been shown to inhibit ATP hydrolysis by ABC transporters [39], another family of ATPases. In addition, *disulfiram* prevented trafficking of the multi-drug resistance protein P-gp to the plasma membrane [40] suggesting that the endosomal pH (controlled primarily by V-ATPases) could be altered in cells treated with *disulfiram*.

The extent of the fluorescence intensity signal detected after addition of 67 μM *disulfiram* to *vma2*Δ cells was greater than anticipated on the basis of pH changes only (Fig. 5) because *vma2*Δ has a vacuolar pH of about 6.9 [17]. A 2.5-fold increase of BCECF fluorescence

intensity would require the pH of the vacuole to start 0.5 pH units lower (pH_{vac} ~ 6.4) and end up at pH 8 in the presence of *disulfiram*.

Vacuoles of V-ATPase null mutants are completely depleted of polyphosphates, which are normally stored in this compartment and buffer the pH [41,42]. Thus, an initial vacuolar pH lower than expected during the experiment is conceivable because the buffering power of the vacuole is lost in *vma2*Δ cells. Yeast vacuolar and cytosolic pH homeostasis are altered in *vma2*Δ [17]. The vacuolar pH of *vma2*Δ changes in response to the extracellular pH and metabolic state of the cells. For example, the vacuolar pH oscillates between 6.5 and 7.1 if *vma2*Δ cells are exposed to medium buffered at pH 5, or pH 7.5 and if extracellular glucose is available or not [17]. In the present study, cells stained with BCECF were resuspended in SD medium (not buffered). Under these conditions, changes at the extracellular medium such as a lower glucose content and pH due to glycolytic activity could produce a drop of the vacuolar pH. It is possible that BCECF itself contributed to reducing the initial pH of the vacuole as well. BCECF was loaded by permeation and hydrolysis of the acetoxymethyl ester group. Products of the deesterification reaction (acetate, formaldehyde, and protons) accumulate and have been shown to lower the pH of the cells over time [43]. In addition, vacuolar BCECF could respond differently to pH changes in wild-type and *vma2*Δ because the pKa of BCECF can be remodeled by the ionic strength of its environment [31].

Regardless of the mechanism by which a high concentration of *disulfiram* can increase fluorescence in V-ATPase deficient cells, this study showed the feasibility of loading yeast vacuoles with BCECF to identify inhibitors of V-ATPase pumps by high throughput screening of chemical libraries. Monitoring of fluorescence intensity changes associated with V-ATPase function is an attractive approach for high throughput screening because of its simplicity and possible outcome. Because pH influences most aspects of cell physiology, V-ATPases are involved in a broad array of cellular processes. The list of human conditions associated with V-ATPase function is growing rapidly [1,3,6–9,12,16] and V-ATPases are emerging as new attractive therapeutic targets [32,44].

Only a small number of specific V-ATPase inhibitors are known [32,44]. They have been used as research tools for the characterization of transport processes in tissues, cells, and purified proteins. These V-ATPase inhibitors are natural products that include three families: concanamycins and bafilomycins, salicylihalamides and lobatamides, and chondropsins [32, 44]. Unfortunately, the supply of these compounds in natural collections is almost exhausted and only few laboratories have developed procedures to synthesize them *in vitro*. For these reasons, most V-ATPase inhibitors are not readily accessible. Only bafilomycin and concanamycin, the most widely used inhibitors, are commercially available.

Future studies will address potential new applications of *disulfiram* as an inhibitor of V-ATPases in yeast and human cell lines that are known to rely on V-ATPase proton transport (kidney, bone, and cancer). We will use this approach for high throughput screening of chemical libraries of small compounds. Screens could lead to the discovery of novel and more accessible V-ATPase inhibitors. Because V-ATPases are highly conserved [1,2], V-ATPase inhibitors can be used as research and therapeutic tools to help define the cellular and molecular mechanisms regulating V-ATPase function and pH homeostasis in yeast and human cells. Novel V-ATPase inhibitors could then be applied towards uncovering the mechanisms controlling human pH homeostasis in cancer, osteoporosis, viral infection, and many other diseases where V-ATPases are involved.

Acknowledgments

This work was supported by NSF CAREER Award MCB-0728833 (to K. J. P.), NIH 1U54MH084690 (to LAS and CA), and CA118100 to the Cancer Center. We thank Drs. Juan Strouse, Catherine Prudom, and other researchers at

the UNMCMD for the helpful discussions. We also thank Dr. Patricia Kane for donating the yeast strains used in this study. Images in this paper were generated in the University of New Mexico Cancer Center Fluorescence Microscopy Facility, supported as detailed on the webpage: http://hsc.unm.edu/crtc/microscopy/Facility.html.

REFERENCES

[1]. Forgac M. Vacuolar ATPases: rotary proton pumps in physiology and pathophysiology. Nat. Rev. Mol. Cell. Biol 2007;8:917–929. [PubMed: 17912264]

[2]. Kane PM. The where, when, and how of organelle acidification by the yeast vacuolar H+-ATPase. Microbiol. Mol. Biol. Rev 2006;70:177–191. [PubMed: 16524922]

[3]. Breton S, Brown D. New insights into the regulation of V-ATPase-dependent proton secretion. Am. J. Physiol. Renal Physiol 2007;292:F1–10. [PubMed: 17032935]

[4]. Yao G, Feng H, Cai Y, Qi W, Kong K. Characterization of vacuolar-ATPase and selective inhibition of vacuolar-H(+)-ATPase in osteoclasts. Biochem Biophys. Res. Commun 2007;357:821–827.

[5]. Karet FE. Physiological and metabolic implications of V-ATPase isoforms in the kidney. J. Bioenerg. Biomembr 2005;37:425–429. [PubMed: 16691477]

[6]. Taranta A, Migliaccio S, Recchia I, Caniglia M, Luciani M, De Rossi G, Dionisi-Vici C, Pinto RM, Francalanci P, Boldrini R, Lanino E, Dini G, Morreale G, Ralston SH, Villa A, Vezzoni P, Del Principe D, Cassiani F, Palumbo G, Teti A. Genotype-phenotype relationship in human ATP6i-dependent autosomal recessive osteopetrosis. Am. J. Pathol 2003;162:57–68. [PubMed: 12507890]

[7]. Stover EH, Borthwick KJ, Bavalia C, Eady N, Fritz DM, Rungroj N, Giersch AB, Morton CC, Axon PR, Akil I, Al-Sabban EA, Baguley DM, Bianca S, Bakkaloglu A, Bircan Z, Chauveau D, Clermont MJ, Guala A, Hulton SA, Kroes H, Li Volti G, Mir S, Mocan H, Nayir A, Ozen S, Rodriguez Soriano J, Sanjad SA, Tasic V, Taylor CM, Topaloglu R, Smith AN, Karet FE. Novel ATP6V1B1 and ATP6V0A4 mutations in autosomal recessive distal renal tubular acidosis with new evidence for hearing loss. J. Med. Genet 2002;39:796–803. [PubMed: 12414817]

[8]. Fais S, De Milito A, You H, Qin W. Targeting vacuolar H+-ATPases as a new strategy against cancer. Cancer Res 2007;67:10627–10630. [PubMed: 18006801]

[9]. Sennoune SR, Luo D, Martínez-Zaguilán R. Plasmalemmal vacuolar-type H+-ATPase in cancer biology. Cell Biochem Biophys 2004;40:185–206. [PubMed: 15054222]

[10]. Lu X, Qin W, Li J, Tan N, Pan D, Zhang H, Xie L, Yao G, Shu H, Yao M, Wan D, Gu J, Yang S. The growth and metastasis of human hepatocellular carcinoma xenografts are inhibited by small interfering RNA targeting to the subunit ATP6L of proton pump. Cancer Res 2005;65:6843–6849. [PubMed: 16061667]

[11]. De Milito A, Iessi E, Logozzi M, Lozupone F, Spada M, Marino ML, Federici C, Perdicchio M, Matarrese P, Lugini L, Nilsson A, Fais S. Proton pump inhibitors induce apoptosis of human B-cell tumors through a caspase-independent mechanism involving reactive oxygen species. Cancer Res 2007;67:5408–5417. [PubMed: 17545622]

[12]. Martínez-Zaguilán R, Raghunand N, Lynch RM, Bellamy W, Martinez GM, Rojas B, Smith D, Dalton WS, Gillies RJ. pH and drug resistance. I. Functional expression of plasmalemmal V-type H+-ATPase in drug-resistant human breast carcinoma cell lines. Biochem. Pharmacol 1999;57:1037–1046. [PubMed: 10796074]

[13]. Kane PM. The long physiological reach of the yeast vacuolar H+-ATPase. J. Bioenerg. Biomembr 2007;39:415–421. [PubMed: 18000744]

[14]. Oka T, Futai M. Requirement of V-ATPase for ovulation and embryogenesis in *Caenorhabditis elegans*. J. Biol. Chem 2000;275:29556–29561. [PubMed: 10846178]

[15]. Davies SA, Goodwin SF, Kelly DC, Wang Z, Sozen MA, Kaiser K, Dow JA. Analysis and inactivation of vha55, the gene encoding the vacuolar ATPase B-subunit in *Drosophila melanogaster* reveals a larval lethal phenotype. J. Biol. Chem 1996;271:30677–30684. [PubMed: 8940044]

[16]. Hinton A, Bond S, Forgac M. V-ATPase functions in normal and disease processes. Pflugers Arch. Eur. J. Physiol 2009;457:589–598. [PubMed: 18026982]

[17]. Martínez-Muñoz GA, Kane P. Vacuolar and plasma membrane proton pumps collaborate to achieve cytosolic pH homeostasis in yeast. J. Biol. Chem 2008;283:20309–20319. [PubMed: 18502746]

[18]. Jefferies KC, Cipriano DJ, Forgac M. Function, structure and regulation of the vacuolar (H+)-ATPases. Arch. Biochem. Biophys 2008;476:33–42. [PubMed: 18406336]

[19]. Arata Y, Baleja JD, Forgac M. The vacuolar (H+)-ATPases-nature's most versatile proton pumps. Nat Rev Mol. Cell. Biol 2002;3:94–103. [PubMed: 11836511]

[20]. Wilkens S. Rotary molecular motors. Adv. Protein Chem 2005;71:345–382. [PubMed: 16230116]

[21]. Edwards BS, Oprea TI, Prossnitz ER, Sklar LA. Flow cytometry for high-throughput, high-content screening. Current Opinion in Chemical Biology 2004;8:392–398. [PubMed: 15288249]

[22]. Young SM, Bologa C, Prossnitz ER, Oprea TI, Sklar LA, Edwards BS. High-throughput screening with HyperCyt flow cytometry to detect small molecule formylpeptide receptor ligands. Journal of Biomolecular Screening 2005;10:374–382. [PubMed: 15964939]

[23]. Zhang JH, Chung TD, Oldenburg KR. A Simple Statistical Parameter for Use in Evaluation and Validation of High Throughput Screening Assays. Journal of Biomolecular Screening 1999;4:67–73. [PubMed: 10838414]

[24]. Owegi MA, Pappas DL Jr, Finch MW, Bilbo SA, Resendiz CA, Jacquemin LJ, Warrier A, Trombley JD, McCulloch KM, Margalef KL, Mertz MJ, Storms JM, Damin CA, Parra KJ. Identification of a domain in the V0 subunit d that is critical for coupling of the yeast vacuolar proton-translocating ATPase. J. Biol. Chem 2006;281:30001–30014. [PubMed: 16891312]

[25]. Owegi MA, Carenbauer AL, Wick NM, Brown JF, Terhune KL, Bilbo SA, Weaver RS, Shircliff R, Newcomb N, Parra-Belky KJ. Mutational analysis of the stator subunit E of the yeast V-ATPase. J. Biol. Chem 2005;280:18393–18402. [PubMed: 15718227]

[26]. Lotscher HR, deJong C, Capaldi RA. Interconversion of high and low adenosinetriphosphatase activity forms of *Escherichia coli* F1 by the detergent lauryldimethylamine oxide. Biochemistry 1984;23:4140–4143. [PubMed: 6237684]

[27]. Drose S, Bindseil K, Bowman EJ, Siebers A, Zeeck A, Altendorf K. Inhibitory effect of modified bafilomycins and concanamycins on P- and V-type adenosinetriphosphatases. Biochemistry 1993;32:3902–3906. [PubMed: 8385991]

[28]. Lowry OH, Rosebrough NJ, Farr AL, Randall RJ. Protein measurement with the Folin phenol reagent. J. Biol. Chem 1951;193:265–275. [PubMed: 14907713]

[29]. Plant PJ, Manolson MF, Grinstein S, Demaurex N. Alternative mechanisms of vacuolar acidification in H(+)-ATPase-deficient yeast. J. Biol. Chem 1999;274:37270–37279. [PubMed: 10601292]

[30]. Ali R, Brett CL, Mukherjee S, Rao R. Inhibition of sodium/proton exchange by a Rab-GTPase-activating protein regulates endosomal traffic in yeast. J. Biol. Chem 2004;279:4498–4506. [PubMed: 14610088]

[31]. Boens N, Qin W, Basarić N, Orte A, Talavera EM, Alvarez-Pez JM. Photophysics of the fluorescent pH indicator BCECF. J. Phys. Chem. A 2006;110:9334–43. [PubMed: 16869681]

[32]. Bowman EJ, Bowman BJ. V-ATPases as drug targets. J. Bioenerg. Biomembr 2005;37:431–435. [PubMed: 16691478]

[33]. Bowman EJ, O'Neill FJ, Bowman BJ. Mutations of pma-1, the gene encoding the plasma membrane H+-ATPase of Neurospora crassa, suppress inhibition of growth by concanamycin A, a specific inhibitor of vacuolar ATPases. J. Bio. Chem 1997;272:14776–14786. [PubMed: 9169444]

[34]. Bowman BJ, Bowman EJ. Mutations in subunit C of the vacuolar ATPase confer resistance to bafilomycin and identify a conserved antibiotic binding site. J. Biol. Chem 2002;277:3965–3972. [PubMed: 11724795]

[35]. Parra KJ, Kane PM. Reversible association between the V1 and Vo domains of yeast vacuolar H+-ATPase is an unconventional glucose-induced effect. Mol. Cell. Biol 1998;18:7064–7074. [PubMed: 9819393]

[36]. Sauna Z, Shukla S, Amdudkar S. Disulfiram, an old drug with new potential therapeutic uses for human cancers and fungal infections. Mol. BioSyst 2005;1:127–134. [PubMed: 16880974]

[37]. Feng Y, Forgac M. Inhibition of vacuolar H(+)-ATPase by disulfide bond formation between cysteine 254 and 532 in subunit A. J. Biol. Chem 1994;269:13224–13230. [PubMed: 8175752]

[38]. Feng Y, Forgac M. A novel mechanism for regulation of vacuolar acidification. J. Biol. Chem 1992;267:19769–19772. [PubMed: 1400289]

[39]. Sauna ZE, Peng XH, Nandigama K, Tekle S, Ambudkar SV. The molecular basis of the action of disulfiram as a modulator of the multidrug resistance-linked ATP binding cassette transporters MDR1 (ABCB1) and MRP1 (ABCC1). Mol. Pharmacol 2004;65:675–684. [PubMed: 14978246]

[40]. Loo TW, Clarke DM. Blockage of drug resistance in vitro by disulfiram, a drug used to treat alcoholism. J Natl Cancer Inst 2000;92:898–902. [PubMed: 10841824]

[41]. Beauvoit B, Rigoulet M, Raffard G, Canioni P, Guerin B. Differential sensitivity of the cellular compartments of *Saccharomyces cerevisiae* to protonophoric uncoupler under fermentative and respiratory energy supply. Biochemistry 1991;30:11212–11220. [PubMed: 1835654]

[42]. Li SC, Kane PM. The yeast lysosome-like vacuole: endpoint and crossroads. Biochim Biophys Acta 2009;1793:650–63. [PubMed: 18786576]

[43]. Aharonovitz O, Fridman H, Livne AA, Granot Y. The effect of BCECF on intracellular pH of human platelets. Biochim. Biophys. Acta 1996;1284:227–232. [PubMed: 8914588]

[44]. Huss M, Wieczorek H. Inhibitors of V-ATPases: old and new players. J. Exp. Biol 2009;212:341–346. [PubMed: 19151208]

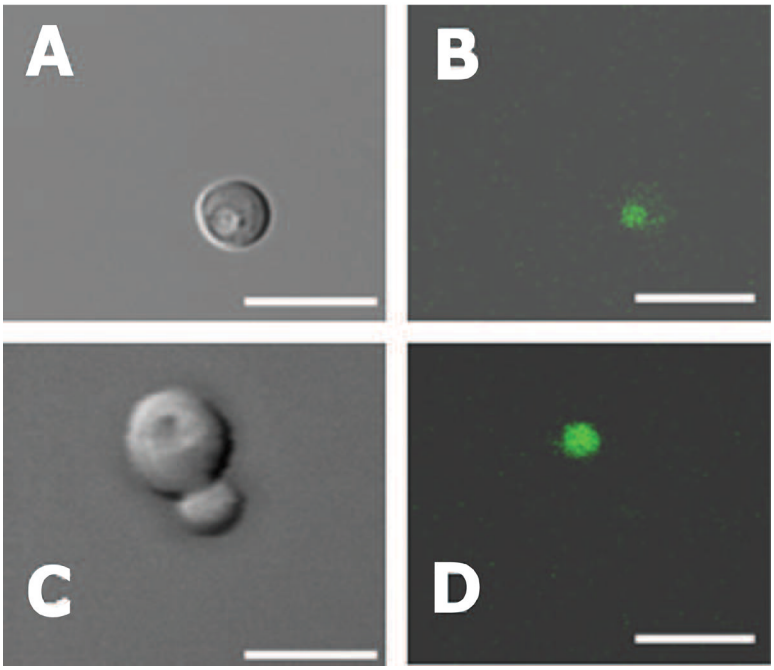

Figure 1. Vacuolar Localization of BCECF in Yeast Cells

Yeast cells were grown overnight to mid-log phase and stained with 18 μM BCECF-AM for 30 min at 30 °C as described under Materials and Methods. Excess BCECF-AM was washed away and cells were resuspended in SD medium (0.5 A_{600}/ml). Photomicroscopy was performed by using a Zeiss LSM 510 confocal microscope with a 63× objective. A and C: Cells observed by differential interference contrast. B and D: Cells were excited at 488 nm and emission read with a 505 nm long pass filter. The same fields were viewed in A – B; and C – D. Shown are wild-type (A, B) and *vma2*Δ (C, D) strains. Scaling bars represent 10 μm.

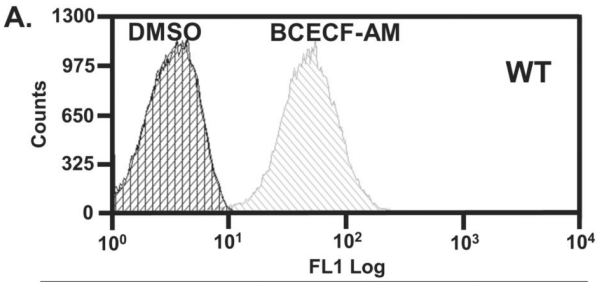

		Counts	Mean	Median
Wild-type	DMSO	40811	3.66	3.29
	BCECF	31865	56.60	47.69
	SD	30372	3.55	3.29

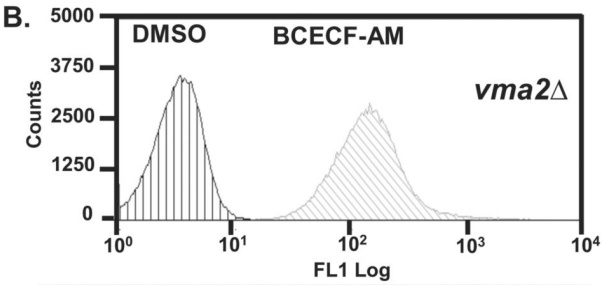

		Counts	Mean	Median
vma2Δ	DMSO	114730	3.66	3.41
	BCECF	108267	202.28	146.12
	SD	-	-	-

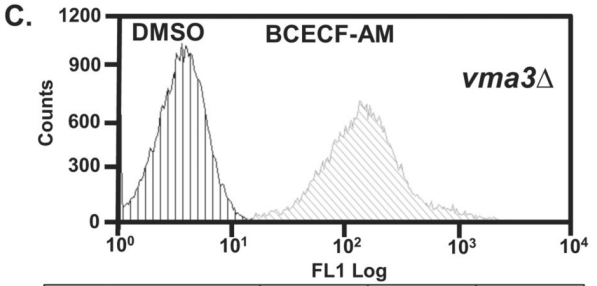

		Counts	Mean	Median
vma3Δ	DMSO	34646	3.96	3.54
	BCECF	18377	247.03	146.12
	SD	-	-	-

Figure 2. Median Channel Fluorescence of Wild-type and V-ATPase Deficient (vma2Δ and vma3Δ) Yeast Cells

Cells were grown overnight to mid-log phase, resuspended in SD media, and treated with 50 μM BCECF-AM in the presence of 1% DMSO or with 1% DMSO alone. Cells were incubated at 30 °C. After 30 min, excess BCECF-AM was washed away and the cells resuspended in SD at a density of 0.25 Abs_{600}/ml for flow cytometry measurements. Cells were sampled with a HyperCyt® autosampler and 2 μl volumes taken and interrogated for BCECF fluorescence using a CYAN ADP (Beckman-Coulter) flow cytometer. After excitation at 488 nm, fluorescence emission was collected using a 530/40 nm filter set. (A) For wild-type cells aliquots of 30μl were distributed into a 384-well plate (48 replicates). The histogram obtained

for an additional population of unlabeled wild-type cells, which received no treatment (SD medium), was superimposed with the histogram of cells treated with DMSO alone. For *vma2*Δ (B) and *vma3*Δ (C) mutants, cells were separately sampled six times from an Eppendorf tube.

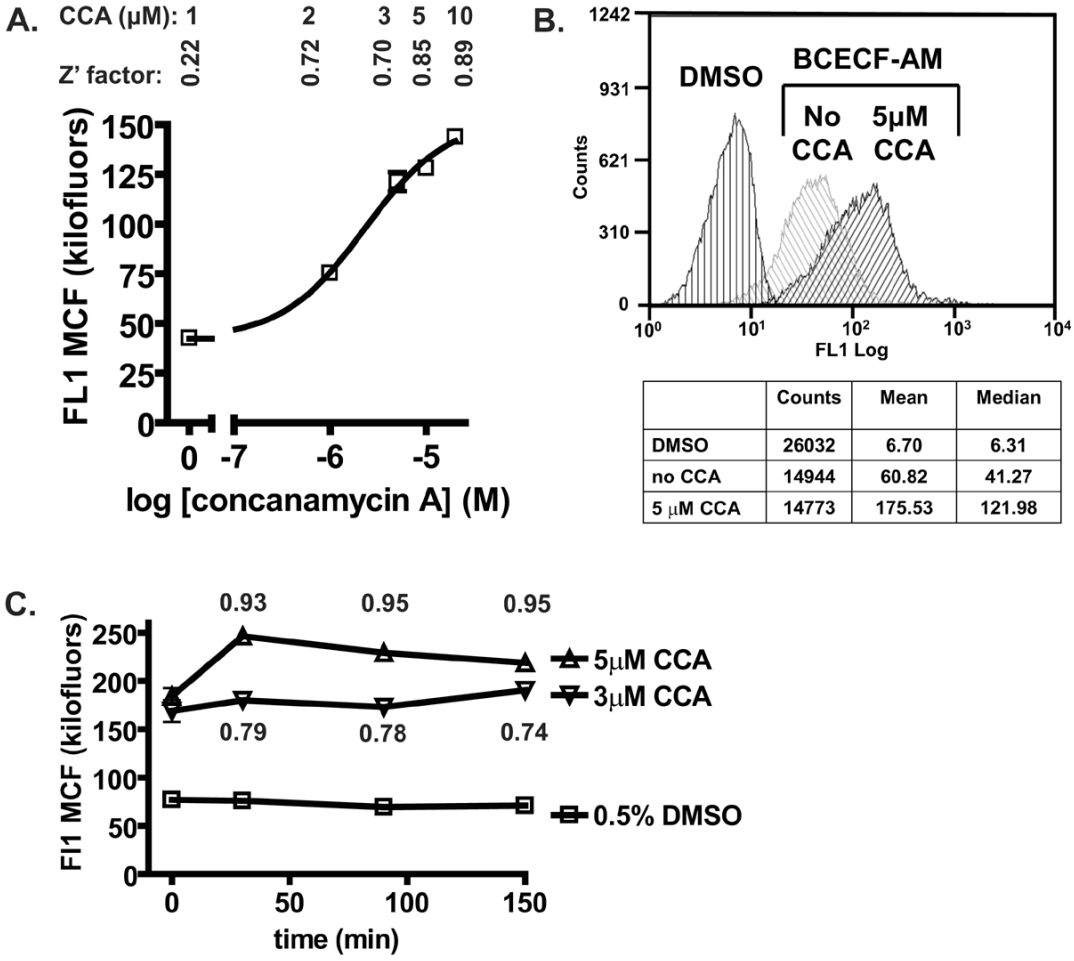

	Counts	Mean	Median
DMSO	26032	6.70	6.31
no CCA	14944	60.82	41.27
5 μM CCA	14773	175.53	121.98

Figure 3. Pharmacological Inhibition of V-ATPase Activity Enhanced BCECF Signals

Concanamycin A dose-response. ***(A)*** Yeast cells stained with BCECF-AM were incubated with varied concentrations of concanamycin A in the presence of 0.5% DMSO for 30 min at 30 ° C. After incubation, cells were harvested, resuspended in an equal concentration of concanamycin A and distributed into 96-well plates (125 μl/well). Cells were sampled with a HyperCyt® autosampler and 2 μl volumes taken and interrogated for BCECF fluorescence as described in the legend to Fig. 2. Shown are the median channel fluorescence (MCF) of the histogram (i.e., the fluorescence intensity) and Z' values at the indicated concentrations of concanamycin A. No additional increment of fluorescence was measured at 20 μM concanamycin A ($MCF_{20\mu M}$=143.9 +/− 2.58; Z'=0.86). Each data point represents the average (+/− STD) of eight replicate wells. ***(B)*** Histograms of unstained and BCECF stained cells before and after treatment with 5 μM concanamycin A. *Concanamycin A time-course.* ***(C)*** BCECF labeled cells (0.25 A_{600}/ml) were treated with the indicated concentrations of concanamycin A containing 0.5% DMSO; or with 0.5 % DMSO alone. Cells were distributed into a 96-well plate and flow cytometry sampling started (t=0). BCECF emission data were collected at 30 min, 90 min, and 150 min incubation at 30 °C on an end-over-end rotator. Each data point represents the average (+/− STD) of four replicate wells (3 μM and 5 μM concanamycin A), and eight replicate wells (0.5% DMSO). The standard deviation between replica measurements was below 5%; these values are mostly contained within the figure symbols. Shown are Z' values at 5 μM and 3 μM concanamycin A. CCA= concanamycin A.

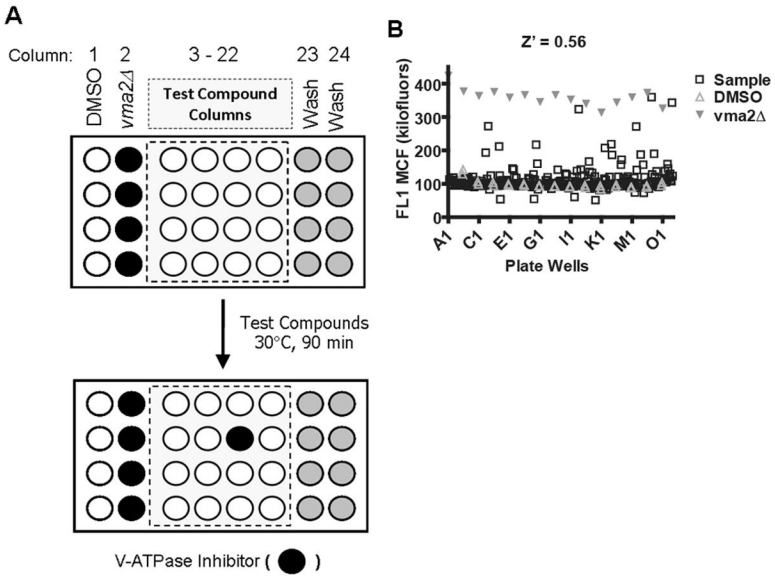

Figure 4. High Throughput Screen of the Prestwick Chemical Library of Small Compounds

(A) Configuration of cells in the microplates during high throughput screening. For three 384-well microplates we configured each with 32 control wells (columns 1 and 2) and 32 wash wells (columns 23 and 24), leaving 320 wells (columns 3 – 22) to which test compounds were added. Controls included *vma2*Δ cells (positive control) and wild-type cells (negative control) each stained with 50 μM BCECF-AM. After addition of test compounds, microplates were incubated at 30 °C for 90 min in an end-over-end rotator. Potential hit compounds were identified as fluorescence signals that mimic *vma2*Δ cell signals. (B) *High Throughput Screen.* BCECF stained wild-type and *vma2*Δ mutant cells were automatically plated into there 384-well plates (15 μl volumes) to which an additional 15 μl of either 0.5% DMSO alone or test compounds were added to a final concentration of 2 mg/ml containing 0.5% DMSO. Shown is one plate high throughput screened for inhibitors of yeast V-ATPase pumps (compounds that enhance fluorescence signals). The X axis displays each well: time bins were automatically drawn around the clusters by using IDLQuery/HyperView software programs, each cluster corresponded to one well. The Y axis displays the amount of fluorescence (FL1 Median Channel Fluorescence).

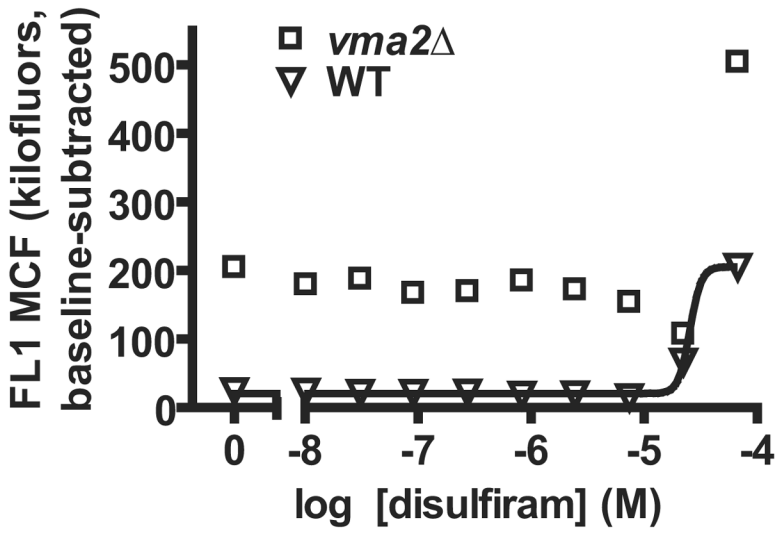

Figure 5. Confirmatory Dose Response Assay

Cells grown to mid-log phase were stained with 50 μM BCECF-AM and 5 μl aliquots distributed into 384-well plates containing varied amounts of the hit compound *disulfiram*. Plates (0.25 OD_{600} cells /μl) were incubated for 90 min at 30 °C. After excitation at 488 nm, fluorescence was collected using a 530/40 nm filter set and a CYAN ADP (Beckman-Coulter) flow cytometer. Data files were processed using IDLQuery/HyperView software programs. The Y axis displays the amount of fluorescence (FL1 Median Channel Fluorescence). WT=wild-type, *vma2*Δ=V-ATPase null mutant cells.

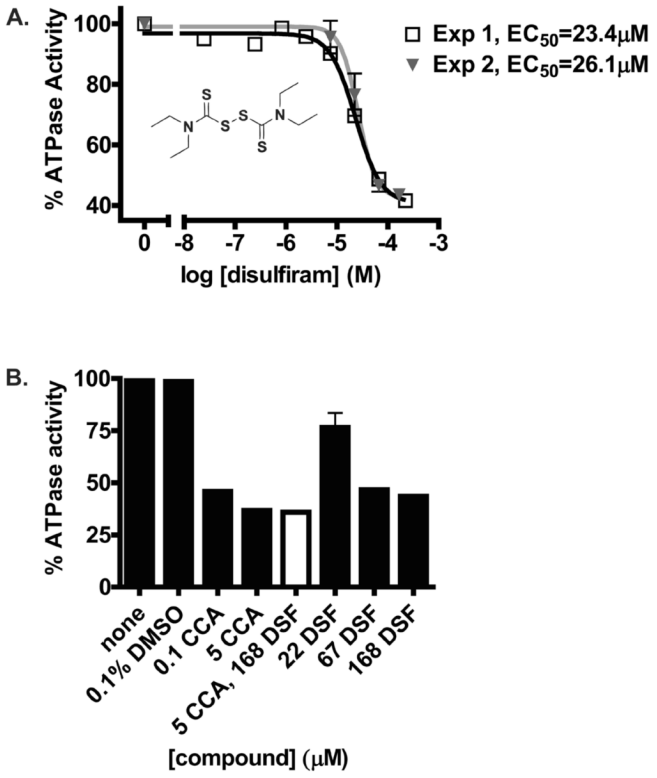

Figure 6. Inhibition of ATP Hydrolysis in Vacuolar Membranes

Vacuolar membranes were purified from wild-type yeast cells by ficoll density gradient centrifugation as described under Materials and Methods [24,25]. (A) Membranes (7 –10 μg protein) were incubated with varied concentrations of disulfiram containing 0.1% DMSO. After 10 min incubation on ice, ATP hydrolysis was measured spectrophotometrically at 37 ° C using an assay coupled to NADH oxidation at 340 mm [26]. The results from two independent experiments using different vacuolar membrane preparations are shown. (B) *Black Bars*: Vacuolar membranes (7 – 10 μg protein) were treated as follows: with concanamycin A (0.1 μM, 5 μM) containing 0.1% DMSO; with disulfiram (22 μM, 67 μM, 168 μM) containing 0.1% DMSO; with 0.1% DMSO alone; or no treatment (*None*). Except for the treatments with 5 μM concanamycin A and 168 μM disulfiram, which involved for 5 min incubations, all other incubations were conducted for 10 min on ice. *White Bar*: Vacuolar membranes (10 μg of protein) were treated with 5 μM concanamycin A for 5 min on ice, after which 168 μM disulfiram was added and membranes incubated on ice for an additional 5 min. The final concentration of DMSO in the mixture was 0.1%. ATP hydrolysis was measured as described under Materials and Methods.

TABLE 1

Comparison of Treatment Conditions Measured by High Throughput Flow Cytometry of Wild-type and vma Mutants.

TREATMENT I		TREATMENT II		Statistical Analysis	Parameter Assessed
Strain[a,b]	**Condition[c]**	**Strain[a,b]**	**Condition**		
WT	BCECF, DMSO	WT	DMSO[d]	5.98 fold[f]	Signal-to-background
vma2 Δ	BCECF, DMSO	*vma2* Δ	DMSO[d]	18.56 fold[f]	Signal-to-background
WT	BCECF, DMSO	*vma2* Δ	BCECF, DMSO[c]	Z' = 0.72[g]	Dynamic range
WT	BCECF, DMSO	WT	BCECF, SD[e]	$p = 0.404$[h]	Effect of DMSO
vma2 Δ	BCECF, DMSO	*vma2* Δ	BCECF, SD[e]	$p = 0.103$[h]	Effect of DMSO

[a] Wild-type strain, contains active V-ATPase pumps.

[b] V-ATPase null mutant strain, lacks V-ATPase function.

[c] Cells were stained with 50 μM BCECF containing 1% DMSO as described under Materials and Methods. After washes, cells were resuspended in 0.5% DMSO.

[d] Cells treated with 1% DMSO alone.

[e] Cells were stained with 50 μM BCECF containing 1% DMSO as described under Materials and Methods. After washes, cells were resuspended in synthetic complete medium (SD).

[f] Fold changes were calculated as the ratio of the mean fluorescence intensity of stained cells divided by the mean fluorescence of unstained cells.

[g] Z' value was calculated by comparing the fluorescence intensity of cells exposed to treatments I and II using the equation described under Materials and Methods.

[h] The treatment with DMSO was statistically indistinguishable from control cells. Student's t test, $p > 0.05$.

Anal Biochem. Author manuscript; available in PMC 2011 March 15.